

VISCOELASTIC PROPERTIES OF DILUTE POLYMER SOLUTIONS

John D. Ferry

Department of Chemistry, University of Wisconsin, Madison, Wisconsin 53706, USA

Abstract - The frequency dependences of the intrinsic storage and loss shear moduli can be predicted from molecular theories for flexible random coil polymers (bead-spring models) and for rigid elongated macromolecules. Comparison with various experimental data extrapolated to infinite dilution shows good agreement with both these extreme types. For semi-rigid helical macromolecules, and for highly charged polyelectrolytes, experimental data correspond to hybrid relaxation spectra which are attributed to rigid-body rotation together with certain internal motions -- probably flexural modes for the helices, configurational rearrangements for the polyelectrolytes. At high frequencies or in high-viscosity solvents, additional energy dissipation mechanisms appear in random coil polymers, whose nature is still conjectural.

INTRODUCTION

The dynamics of isolated polymer molecules have been extensively treated theoretically in recent years (1,2). Experimental data on dilute solutions are being provided from various sources, including viscoelastic properties, dielectric and nuclear magnetic resonance relaxation, and quasielastic light scattering. Of these, the first has furnished information on the motions of a wide variety of macromolecules. This review emphasizes viscoelasticity studies which have been completed since the earlier comprehensive review by Osaki (3).

Dynamic viscoelastic measurements on dilute polymer solutions in the audiofrequency range in low-viscosity solvents provide information on motional modes associated with relatively long relaxation times (e.g., 10^{-4} s). Most of the data cited here were obtained with the Birnboim-Schrag multiple-lumped resonator (4) in the frequency range from 100 to 8000 Hz. Shorter-range motions with smaller relaxation times can be probed at higher frequencies as by Wada and collaborators (5) or in high-viscosity solvents such as chlorinated diphenyls, for example in the modified Birnboim transducer apparatus (6).

THEORY

When a viscoelastic material is subjected to small sinusoidally oscillating shearing deformations, the in-phase and out-of-phase stress/strain ratios are termed the storage (G') and loss (G'') shear moduli. Theories based on models for the motion of isolated molecules predict the ratios of these moduli to weight concentration (c) extrapolated to infinite dilution, viz.

$$[G'] = \lim_{c \rightarrow 0} G'/c, \quad [G''] = \lim_{c \rightarrow 0} (G'' - \omega\eta_s)/c \quad (1)$$

in which the solvent contribution to the loss modulus, $\omega\eta_s$, has been subtracted; ω is the radian frequency of deformation and η_s the solvent viscosity. The intrinsic moduli $[G']$ and $[G'']$ can be converted to the dimensionless reduced moduli $[G']_R$ and $[G'']_R$ by multiplying by M/RT , where M is molecular weight (usually uniform, but if not, number-average), and the theoretical predictions are most conveniently expressed in this form.

Flexible random coils

The theory of Zimm (7) is based on the bead-spring model for a linear molecule, according to which the molecule is divided into N submolecule springs (a large number), each of which stores elastic energy due to changes in configurational entropy when distorted, while frictional resistance to motion through the solvent is concentrated at the submolecule junctions (beads). It predicts

$$[G']_R = \sum_{p=1}^N \omega^2 \tau_p^2 / (1 + \omega^2 \tau_p^2) \quad (2)$$

$$[G'']_R = \sum_{p=1}^N \omega \tau_p / (1 + \omega^2 \tau_p^2) \quad (3)$$

If N is large, the results are insensitive to N except at very high frequencies. The longest relaxation time τ_1 corresponds to a mode of configurational change in which the ends of the molecule are moving in opposite directions; it is related to measurable quantities by

$$\tau_1 = [\eta] \eta_s M / RT S_1 \quad (4)$$

where $[\eta]$ is the intrinsic viscosity (low-frequency limiting value of $[G'']/\omega \eta_s$) and $S_1 = \sum \tau_p / \tau_1 = 2.37$. The other relaxation times τ_p correspond to more complicated motional modes and their ratios τ_p/τ_1 are obtained from eigenvalues of a matrix which describes the forces on the beads. The frequency dependences of $[G']_R$ and $[G'']_R$ are portrayed in Fig. 1. The dimensionless frequency used here is convenient for comparison with experimental data.

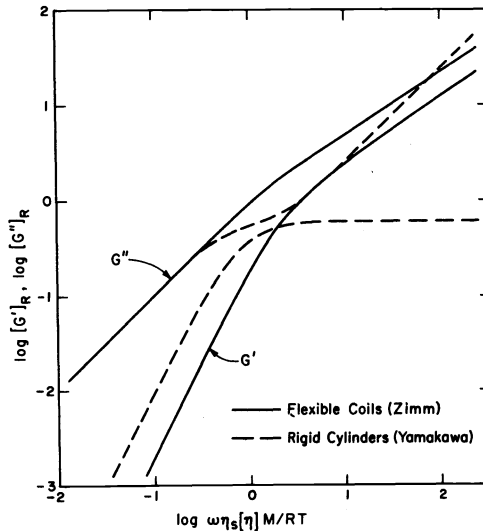


Fig. 1. Reduced intrinsic shear moduli $[G']_R$ and $[G'']_R$ plotted logarithmically against dimensionless frequency $\omega \eta_s [\eta] M / RT$ for flexible random coils (Zimm theory) and rigid cylinders (Yamakawa theory with very high length/diameter ratio).

The original theory is applicable to solutions in Θ solvents. For other than Θ solvents, the theory can be modified with introduction of a hydrodynamic interaction parameter which changes the form of the frequency dependence somewhat and can be determined empirically by matching to experimental data; it appears to be inversely proportional to the linear expansion factor in good solvents (3). Also, the theory can be modified to describe branched molecules with star and certain regular comb structures. Branching changes the form of the frequency dependence and diminishes the magnitude of $[G']_R$ at low frequencies (8-10).

Rigid elongated macromolecules

Several theories for rigid molecules (cylinder, ellipsoid, linear array of beads) predict

$$[G']_R = m_1 \omega^2 \tau_0^2 / (1 + \omega^2 \tau_0^2) \quad (5)$$

$$[G'']_R = \omega \tau_0 [m_1 / (1 + \omega^2 \tau_0^2) + m_2] \quad (6)$$

$$\tau_0 = m [\eta] \eta_s M / RT \quad (7)$$

Here m_1 and m_2 are numerical coefficients which depend slightly on the details of the model, and $m = 1/(m_1 + m_2)$. For cylinders of very high length/diameter ratio L/d , the theory of Yamakawa (11) gives $m_1 = 3/5$, $m_2 = 1/5$. (If L/d is not extremely large, $m_2 > 1/5$ and it depends on L/d .) The same result for large L/d was obtained for a linear array of beads (centers of frictional resistance) by Kirkwood and Auer (12). In Eqs. 5 and 6, there is a

single relaxation time which corresponds to end-over-end rotation of the molecule. The frequency dependences for a very long rigid cylinder are also shown in Fig. 1, and are quite different from those for a flexible random coil. Moreover, the relaxation time τ_0 can be calculated from the dimensions of the molecular model. For example, for the cylinder of Yamakawa,

$$\tau_0 = \pi \eta_s L^3 F_1 / 18kT \quad (8)$$

where L is the length and F_1 is a complicated function of L/d ; when L/d is very large, F_1 can be approximated by $[\ln(L/d)]^{-1}$.

Semirigid elongated macromolecules and highly charged polyelectrolytes: hybrid spectrum
For several macromolecules with characteristics intermediate between those of flexible random coils and rigid rods, it has been found empirically that the frequency dependence of $[G']_R$ and $[G'']_R$ can be described by a hybrid relaxation spectrum consisting of one longest relaxation time (τ_0) together with a set of shorter times (τ_1, τ_2 , etc.) whose spacings correspond to the ratios given by the Zimm theory (13, 14). This specifies

$$[G']_R = m_1 \omega^2 \tau_0^2 / (1 + \omega^2 \tau_0^2) + zZ'(\omega \tau_1) \quad (9)$$

$$[G'']_R = \omega \tau_0 [m_1 / (1 + \omega^2 \tau_0^2) + m_2] + zZ''(\omega \tau_1) \quad (10)$$

where Z' and Z'' are the reduced intrinsic moduli given by Eqs. 2 and 3 and z is a weighting factor, in practice set equal to unity. The longest time τ_0 is still given by Eq. 7 with $m = (m_1 + m_2 + S_1 z \tau_1 / \tau_0)^{-1}$. The ratio τ_0 / τ_1 as well as m_1 and m_2 are taken as adjustable parameters. The relaxation time τ_0 is attributed to end-over-end rotation of the molecule; the others are attributed to some kind of internal motions which may differ depending on the nature of the molecule and may not necessarily be the configurational changes characteristic of the bead-spring model, as will become apparent in the description of experimental results.

High-frequency behavior of flexible random coils

When the product of frequency and solvent viscosity is large, the sinusoidal deformations interact with short-range internal motions which cannot be described in terms of the bead-spring model. Theory here is much more complicated and less well developed but will be mentioned briefly in connection with experimental results.

EXPERIMENTAL RESULTS

Flexible random coils

Data for linear flexible coil polymers have been well reviewed by Osaki (3). In both Θ and good solvents, agreement with the Zimm theory is good, with reasonable choices of the hydrodynamic interaction parameter. For star-shaped molecules with 4 or 9 branches, agreement with the Zimm-Kilb theory (8) as evaluated by Osaki and Schrag (9) is also good, especially if a small correction is made for molecular weight distribution (15). For comb-shaped polymers, the calculation based on the bead-spring model is less satisfactory (16), probably because of a dense concentration of polymer segments near the center of such a molecule. Some data on randomly branched polymers (17, 18) indicate that a very small amount of long-chain branching can be detected by viscoelastic measurements if the molecular weight distribution is narrow. At high frequencies, all flexible coil polymers show deviations from bead-spring model theory which will be mentioned in a separate section.

Rigid elongated macromolecules

The first molecule which was found to display rigid rod behavior was tobacco mosaic virus (19), molecular weight 3.9×10^7 , length 3000\AA , diameter 180\AA , whose rodlike shape is clearly evident in electron micrographs. Logarithmic plots of $[G']_R$ and $[G'']_R$ against $\omega \eta_s M / RT$ are shown in Fig. 2, and the agreement with Eqs. 5 and 6 is reasonably good within experimental uncertainty. In this case, the value of $[\eta]$ needed to match the abscissas of Figs. 1 and 2 was taken from the literature (27 ml/g).

Tobacco mosaic virus aggregates spontaneously end-to-end when aged. Similar measurements on an aggregated sample with a number-average degree of polymerization of 3.6 also agreed very well with the theory, although because of a much larger relaxation time (note the dependence of τ_0 on molecular length in Eq. 8) the data covered only the frequency region well to the right of the inflection in $[G'']_R$. These results confirm the theoretical value of 3/5 for m_1

and also that the end-to-end aggregates are highly rigid (especially in contrast to the results for semirigid molecules to be discussed below).

Oligomers of fibrin, prepared by thrombin-induced polymerization of fibrinogen in the presence of 1,6-hexanediol, which prevents the polymerization from progressing to the ultimate 3-dimensional fibrin clot, have also been studied (20). The frequency dependence of $[G']_R$ and $[G'']_R$ agreed with the predictions of the Yamakawa theory with a relaxation time $\tau_0 = 1.25 \times 10^{-3}$ s reduced to the viscosity of water at 20°. A structure frequently postulated for this oligomer is a lateral dimerization of fibrin units with staggered overlapping leading to two parallel end-to-end chains with an average degree of polymerization of about 20, a length of 4600Å, and a diameter 60Å. For such a model, τ_0 calculated from Eq. 8 is 1.4×10^{-3} s, in quite good agreement. Again, the oligomer appears to have a very rigid structure, reinforced no doubt by the staggered overlapping.

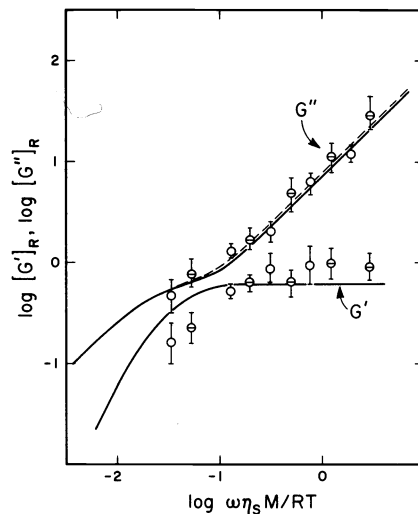


Fig. 2. Logarithmic plots of $[G']_R$ and $[G'']_R$ against $\omega\eta_s M/RT$ for tobacco mosaic virus in a glycerol-water mixture, compared with the Kirkwood-Auer theory, Eqs. 5-7 with $m_1 = 3/5$, $m_2 = 1/5$ (solid curves). Open circles, measurements at 37.8°C, slotted circles at 25.0°C. (Dashed line is theory for elongated ellipsoid model.) (19)

Semi-rigid elongated macromolecules

Poly(γ -benzyl-L-glutamate), in certain solvents, has an extended helical structure, but it is evident from measurements of intrinsic viscosity, light scattering, and dielectric dispersion that the helix is not absolutely straight; it has enough flexibility to be distorted by thermal motions, to an extent that increases with molecular length. Viscoelastic measurements (13) on a sample with weight-average molecular weight 570,000 in two heliogenic solvents with different viscosities are illustrated in Fig. 3. The frequency dependence does not follow either of the extreme types shown in Fig. 1 but is fitted exceedingly well by the hybrid model of Eqs. 9 and 10 with the values of the parameters shown in the legend of the figure. Similar behavior was found for two other samples of lower molecular weights.

Measurements by Wada and collaborators (21) on samples of still lower molecular weights at higher frequencies, extrapolated to infinite dilution, were analyzed in a somewhat similar manner in terms of a long relaxation time attributed to end-over-end rotation together with shorter relaxation times attributed to internal motions. They combined the data of Refs. 13 and 21 with some other non-mechanical data to plot τ_0 logarithmically against molecular weight in Fig. 4. The relaxation time τ_0 is nearly proportional to M^3 (or L^3) and agrees extremely well with the calculation from molecular dimensions from the Kirkwood-Auer theory (Ref. 12, very similar to Eq. 8). This leaves no doubt that the longest relaxation time is associated with end-over-end rotation. The other relaxation mechanisms will be discussed below.

Poly(*n*-hexyl isocyanate) is another synthetic helical molecule which is highly extended but evidently somewhat flexible. For molecular weight 99,000, in Tetralin and Tetralin-Aroclor solvent mixtures, viscoelastic data were in close agreement with the hybrid spectrum of Eqs.

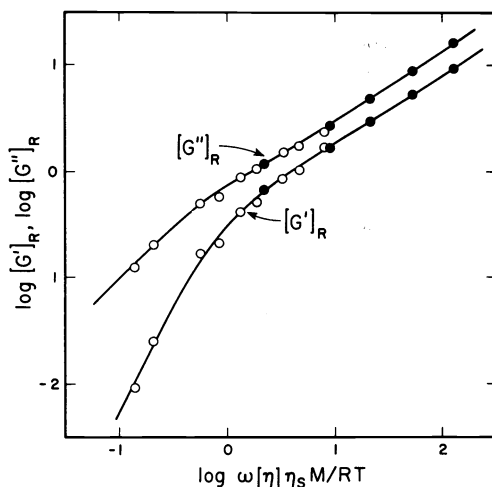


Fig. 3. Logarithmic plots of $[G'']_R$ and $[G']_R$ against $\omega \eta_s [\eta] M/RT$ for poly(γ -benzyl-L-glutamate) ($M_w = 570,000$) in dimethyl formamide (open circles) and *m*-cresol (black circles). Curves drawn from Eqs. 9 and 10 with $m_1 = 0.555$, $m_2 = 0$, $z = 1$, and $\tau_0/\tau_1 = 4.7$ (13).

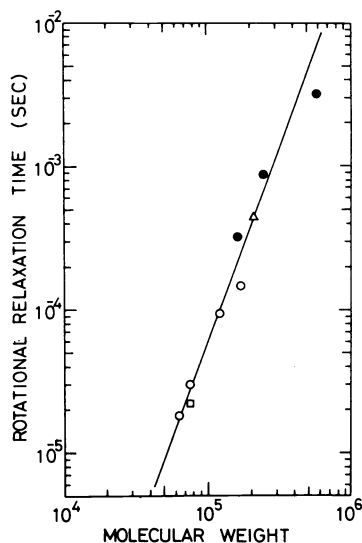


Fig. 4. Logarithmic plot of τ_0 against molecular weight for poly(γ -benzyl-L-glutamate) in *m*-cresol at 25°. Open circles, Ref. 21; black circles, Ref. 13; square, from dielectric data, Ref. 22; triangle, from birefringence data, Ref. 23. Line calculated from molecular dimensions by Kirkwood-Auer theory (12), similar to Eq. 8. (From Ref. 21)

9 and 10; in this case, $m_1 = 0.25$, $m_2 = 0$, $z = 1$, and $\tau_0/\tau_1 = 8.6$ (24). At higher molecular weights, the behavior more nearly resembled that of flexible coils, suggesting that this helix is less rigid than that of poly(γ -benzyl-L-glutamate).

Paramyosin is a rod-like biomacromolecule consisting of two α helices coiled around each other, length 1180Å, diameter 16Å. Data for $[G']_R$ and $[G'']_R$ were closely fitted by Eqs. 9 and 10 with $m_1 = 0.6$, $m_2 = 0.1$, $z = 1$, and $\tau_0/\tau_1 = 8.43$ (14). It is not clear why in this case m_2 is non-zero, but this may be related to the more elaborate structure of the two associated helices as contrasted with the single-helix molecules for which $m_2 = 0$.

Nature of internal motions in semirigid molecules. The relaxation mechanisms with shorter times in the hybrid spectrum have been attributed to some kind of internal motions. The slopes of the $[G']_R$ and $[G'']_R$ curves at high frequencies in Fig. 3 and the spacing between them clearly correspond to a set of relaxation times with Zimm-like spacings, but that does not mean that the motions necessarily resemble those of flexible random coils, where elastic energy is stored due to changes in configurational entropy; other modes might have similar ratios of relaxation times. For helical molecules, plausible internal motions are flexure, and elongation either by accordion-like extension or by untwisting.

Wada and collaborators (21) have calculated the relaxation time for the fundamental flexural mode of a rodlike molecule as

$$\tau_F = 5.53 \times 10^{-3} \eta_s L^4 / B \ln(L/d) \quad (11)$$

where B, the flexural rigidity, is a conventional measure of the resistance to bending. Rosser (25) has calculated the relaxation time for the fundamental extensional mode as

$$\tau_L = \eta_s L^2 / d^2 E \ln(L/d) \quad (12)$$

where E is Young's modulus of the rod. Since τ_0 is approximately proportional to L^3 (Eq. 8), it would be expected that with increasing molecular weight the spacing between τ_L and τ_0 would widen, whereas the spacing between τ_F and τ_0 would narrow and τ_F would eventually overtake τ_0 so that the rotational relaxation would no longer be identifiable. The latter behavior is actually observed in poly(n-hexyl iso-cyanate) and is beginning to be apparent for poly(γ -benzyl-L-glutamate) in the last point in Fig. 4 which deviates from the prediction for the rigid rod as pointed out by Wada (21). It seems very probable, therefore, that the internal motions are flexural.

By combining Eqs. 8 and 11, Wada (21) obtained the convenient equation

$$B \approx 0.10 LkT\tau_0/\tau_F \quad (13)$$

and, if τ_F can be identified with τ_1 of the hybrid spectrum, we calculate for paramyosin $B = 4.0 \times 10^{-19}$ dyn/cm² at 20°C. For poly(γ -benzyl-L-glutamate), Wada calculated 5×10^{-19} dyn/cm² from persistence length data. From B, assuming a cylindrical rod of uniform structure, one can obtain Young's modulus:

$$E = 64B/\pi d^4 \quad (14)$$

For paramyosin, $E = 1.2 \times 10^{10}$ dyn/cm², a rather high value corresponding to that of a polymer in the glassy state. The fact that the molecule is flexible, in spite of the high calculated modulus, reflects its small diameter and small d/L ratio. On the other hand, if E were calculated from Eq. 11 by identifying τ_1 with τ_L , an unreasonably small value of 6.5×10^6 dyn/cm² would be obtained. A molecule with this low modulus would bend so easily that it would scarcely appear rigid.

Polyelectrolytes

A highly charged polyelectrolyte in aqueous solution at low ionic strength has a very extended configuration due to electrostatic repulsion, as shown by intrinsic viscosity and light scattering, but would not be expected to have as much rigidity as the helical macromolecules discussed above. Viscoelastic measurements on the sodium salt of the strong electrolyte poly(styrene sulfonic acid) have been made in glycerol-water mixtures of various dielectric constants and at various ionic strengths (26). Extrapolation to infinite dilution necessitates dialysis of each solution against a solvent of fixed ionic strength to maintain constant chemical potential of the salt component of low molecular weight (27). An example of the frequency dependence of $[G']_R$ and $[G'']_R$ is shown in Fig. 5. It can be fitted very well with the hybrid model of Eqs. 9 and 10 with the values of the parameters shown in the legend of the figure. Similar behavior was found for another sample of higher molecular weight and also at different glycerol and sodium ion concentrations. The ratio τ_0/τ_1 decreases with increasing molecular weight and increasing glycerol concentration; τ_0 increases with increasing molecular weight, decreasing Na⁺ concentration, and (after correction for viscosity difference) with decreasing glycerol concentration.

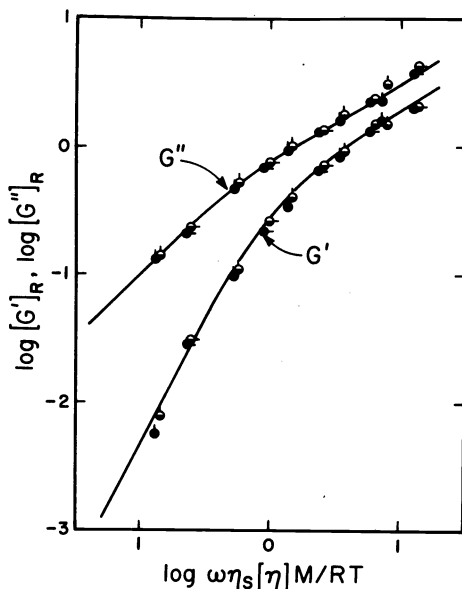


Fig. 5. Logarithmic plots of $[G']_R$ and $[G'']_R$ against $\omega \eta_s [\eta] M / RT$ for sodium poly(styrene sulfonate), molecular weight 3.3×10^5 , in 25% aqueous glycerol. Na^+ concentrations from trisodium salt of ethylene diamine tetraacetic acid: points half black, 0.002M; full black, 0.005M. Pip right, 1.0°C ; up, 15.0°C . Curves drawn from Eq. 9 and 10 with $m_1 = 0.6$, $m_2 = 0$, $z = 1$, and $\tau_0/\tau_1 = 4.0$ (26).

The longest relaxation time τ_0 is again attributed to end-over-end rotation of the molecule in its highly elongated shape. A rough calculation from Eq. 8 of the molecular length based on a cylindrical model gives a value (for aqueous solvent without glycerol) of the order of half the maximum extended contour length of the polymer backbone (0.6 for $M_n = 3.3 \times 10^5$, 0.4 for $M_n = 7.8 \times 10^5$) showing that the elongation is indeed extreme. However, values of τ_0 for two molecular weights correspond to a proportionality to $M^{1.7}$, considerably less dependence than for a fully extended rod. The shorter relaxation times are attributed to modes of configurational change similar to those occurring in uncharged flexible random coils.

Earlier measurements by Wada and collaborators (28) on the weak electrolyte poly(acrylic acid) neutralized to different extents reached rather similar conclusions. These measurements were made at finite polymer concentration, mostly 1.6 g/l. In this case the degree of neutralization is an additional variable. The magnitude of the longest relaxation time (identifiable with τ_0) is plotted against degree of neutralization in Fig. 6. With decreasing neutralization, the magnitude of τ_0 drops and it finally disappears. At complete neutralization, it was found that τ_0 was approximately proportional to M^3 . There are several possible reasons for the difference between this exponent and the smaller one of 1.7 found for poly(styrene sulfonate), the most likely (25) being that the poly(acrylate) data were not extrapolated to infinite dilution and the concentration dependence may increase rapidly with increasing molecular weight (29).

Experiments by Wada and collaborators on poly(methacrylic acid) neutralized to different extents (30) also indicate the presence of a hybrid relaxation spectrum at high degrees of neutralization. At low degrees of neutralization, the molecular configuration is influenced by hydrophobic interaction of the methyl groups.

High-frequency behavior of flexible random coils

The discussion of flexible coils above refers to frequencies which are not too high compared with τ_1^{-1} ; the product $\omega \tau_1$ must be below a figure which increases with increasing molecular weight and for $M = 10^6$ is of the order of 100. At higher frequencies (or higher solvent viscosities) divergences appear which are illustrated in Fig. 7; $G'' - \omega \eta_s$ goes through an inflection and at high frequencies becomes directly proportional to ω (slope of unity on logarithmic plot). Such measurements have usually been made at somewhat higher concentrations

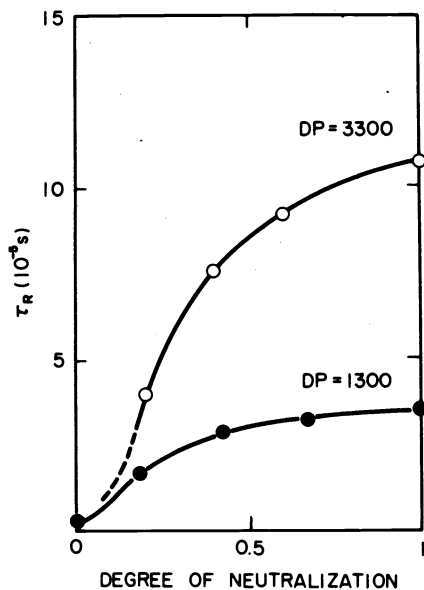


Fig. 6. Plot of rotational relaxation time against degree of neutralization for poly(acrylic acid) with two degrees of polymerization as shown. NaCl concentrations 0.01 M (DP = 1300), 0.021 M (DP = 3300). (28)

than the low-frequency measurements described above, and extrapolation to infinite dilution has been made only in the high-frequency region where the concentration dependence is relatively slight (31-34).

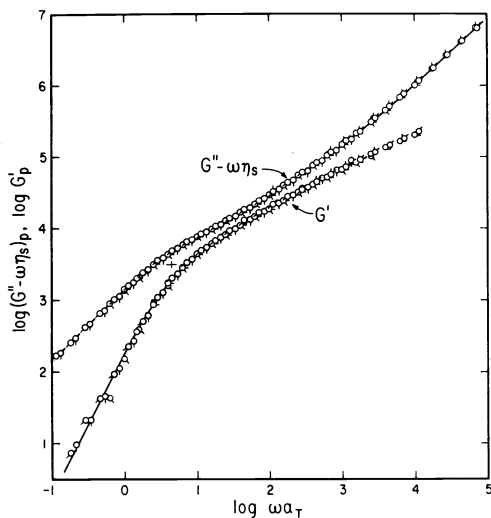


Fig. 7. Logarithmic plots of G' and $G'' - \omega\eta_s$ reduced to 25.0°C. for polystyrene, $M = 2.67 \times 10^5$, in chlorinated diphenyl solvent, concentration 55.4 g/l. Pips refer to measurements at different temperatures from 9.9 to 34.9°C. The shift factor a_T was determined empirically (32).

The proportionality of $G'' - \omega\eta_s$ to ω implies that the dynamic viscosity, $\eta' \equiv G''/\omega$, becomes independent of ω at high frequencies and levels off at a value η'_∞ greater than η_s , corresponding to a finite high-frequency intrinsic dynamic viscosity $[\eta']_\infty$. The latter can be obtained as the slope of a plot of $\ln(\eta'/\eta_s)$ against c (32). It is independent of molecular weight, and for polystyrene (33) it is also independent of branching (both star and comb shapes). However, for different polymers it depends considerably on the chemical structure (34,35). (At extremely high frequencies, there is some evidence (3) that $[\eta']$ attains another lower plateau, so that the designation $[\eta']_\infty$ may be ambiguous.)

The Zimm theory and the modifications of it which have been mentioned, including the hybrid spectrum when $m_2 = 0$, predict that $[\eta']_\infty = 0$, but they are obviously inapplicable at

frequencies which interact with local motions within the fictitious submolecules. A finite $[\eta']_\infty$ implies that there is an additional mechanism for energy dissipation besides that described by the frictional resistance of the beads in the bead-spring model. Several important theoretical treatments of this phenomenon have recently been completed (36-42), but since the subject is developing rapidly at the present time it is inappropriate to review it here.

It was observed by Lamb and Matheson (43) that finite-concentration plots of G' and $G'' - \omega\eta_1$ against frequency, where η_1 was an empirically chosen viscosity higher than η_s , corresponded to the frequency dependence predicted by the bead-spring theory with no hydrodynamic interaction (Rouse theory, Ref. 44). Recently, Schrag has analyzed an extensive series of viscoelastic data by plotting G' and $G'' - \omega\eta'_\infty$ against frequency, where η'_∞ is determined experimentally. The resulting frequency dependence appears to be independent of molecular weight and concentration over considerable ranges and corresponds to the bead-spring theory with very little or no hydrodynamic interaction (45). The significance of this behavior has not yet been resolved.

CONCLUSIONS

Viscoelastic measurements clearly distinguish molecular motions characteristic of flexible random coils, rigid rod-like structures, and elongated macromolecules with partial flexibility. The latter include helical molecules and polyelectrolytes. The internal motions detected in helical molecules appear to be flexural, and a micro-Young's modulus can be calculated from experimental data. In strong polyelectrolytes and fully neutralized weak polyelectrolytes, the internal motions are probably configurational changes similar to those in uncharged polymers. At high frequencies, flexible random coils show additional energy dissipation which is not yet well understood.

Acknowledgment - Much of the work in our laboratory described here was supported by grants from the National Institutes of Health (HL 13760, GM 21652). The permission of Professor Y. Wada to reproduce Figs. 4 and 6 is gratefully acknowledged.

REFERENCES

1. M. Bixon, *Ann. Rev. Phys. Chem.*, **27**, 65 (1976).
2. R. B. Bird, O. Hassager, R. C. Armstrong, and C. F. Curtiss, *Dynamics of Polymeric Liquids*, Vol. II, Wiley, New York (1977).
3. K. Osaki, *Adv. Polymer Sci.*, **12**, 1 (1973).
4. J. L. Schrag and R. M. Johnson, *Rev. Sci. Instr.*, **42**, 224 (1971).
5. H. Nakajima, H. Okamoto, and Y. Wada, *Polymer J.*, **5**, 268 (1973).
6. D. J. Massa and J. L. Schrag, *J. Polymer Sci.*, A-2, **10**, 71.
7. B. H. Zimm, *J. Chem. Phys.*, **24**, 269 (1956).
8. B. H. Zimm and R. W. Kilb, *J. Polymer Sci.*, **37**, 19 (1959).
9. K. Osaki and J. L. Schrag, *J. Polymer Sci.*, *Polymer Phys. Ed.*, **11**, 549 (1973).
10. K. Osaki, Y. Mitsuda, J. L. Schrag, and J. D. Ferry, *Trans. Soc. Rheol.*, **18**, 395 (1973).
11. H. Yamakawa, *Macromolecules*, **8**, 339 (1975).
12. J. G. Kirkwood and P. L. Auer, *J. Chem. Phys.*, **19**, 281 (1951).
13. T. C. Warren, J. L. Schrag, and J. D. Ferry, *Biopolymers*, **12**, 1905 (1973).
14. R. W. Rosser, J. L. Schrag, J. D. Ferry, and M. Greaser, *Macromolecules*, **10**, in press.
15. Y. Mitsuda and J. D. Ferry, *Kobunshi Ronbunshu*, **31**, 135 (1974).
16. Y. Mitsuda, J. L. Schrag, and J. D. Ferry, *Polymer J.*, **4**, 668 (1973).
17. Y. Mitsuda, J. L. Schrag, and J. D. Ferry, *J. Appl. Polymer Sci.*, **18**, 193 (1974).
18. N. Nemoto, Y. Mitsuda, J. L. Schrag, and J. D. Ferry, *Macromolecules*, **7**, 253 (1974).
19. N. Nemoto, J. L. Schrag, J. D. Ferry, and R. W. Fulton, *Biopolymers*, **14**, 409 (1975).
20. N. Nemoto, F. H. M. Nestler, J. L. Schrag, and J. D. Ferry, *Biopolymers*, in press.
21. N. Ookubo, M. Komatsubara, H. Nakajima, and Y. Wada, *Biopolymers*, **15**, 929 (1976).
22. A. Wada and H. Kihara, *Polymer J.*, **3**, 482 (1972).
23. H. Ohe, H. Watanabe, and K. Yoshioka, *Kolloid-Z.Z. Polym.*, **252**, 26 (1964).
24. N. Nemoto, J. L. Schrag, and J. D. Ferry, *Polymer J.*, **7**, 195 (1975).
25. R. W. Rosser, Ph.D. Thesis, University of Wisconsin, 1977.
26. R. W. Rosser, N. Nemoto, J. L. Schrag, and J. D. Ferry, *J. Polymer Sci.*, *Polymer Phys. Ed.*, to be submitted.
27. E. F. Casassa and H. Eisenberg, *J. Phys. Chem.*, **64**, 753 (1960).
28. H. Okamoto, H. Nakajima, and Y. Wada, *J. Polymer Sci.*, *Polymer Phys. Ed.*, **12**, 1035 (1974).
29. M. Doi, *J. Phys.*, **36**, 607 (1975).

30. H. Okamoto and Y. Wada, J. Polymer Sci., Polymer Phys. Ed., 12, 2413 (1974).
31. D. J. Massa, J. L. Schrag, and J. D. Ferry, Macromolecules, 4, 210 (1971).
32. K. Osaki and J. L. Schrag, Polymer J., 2, 541 (1971).
33. J. W. M. Noordermeer, O. Kramer, F. H. M. Nestler, J. L. Schrag, and J. D. Ferry, Macromolecules, 8, 539 (1975).
34. J. W. M. Noordermeer, J. D. Ferry, and N. Nemoto, Macromolecules, 8, 672 (1975).
35. B. J. Cooke and A. J. Matheson, Faraday Trans. II, 3, 679 (1976).
36. J. T. Fong and A. Peterlin, J. Res. Nat. Bur. Standards, 80B, 273 (1976).
37. P. G. de Gennes, J. Phys., in press.
38. K. Freed, J. Chem. Phys., in press.
39. M. Fixman and J. Kovac, J. Chem. Phys., 61, 4939, 4950 (1974).
40. M. Fixman, private communication.
41. D. A. MacInnes, J. Polymer Sci., Polymer Phys. Ed., 15, 465, 657 (1977).
42. R. Cerf, J. Phys., 38, 357 (1977).
43. J. Lamb and A. J. Matheson, Proc. Roy. Soc., A281, 207 (1964).
44. P. E. Rouse, Jr., J. Chem. Phys., 21, 1272 (1953).
45. B. G. Brueggeman, M. G. Minnick, and J. L. Schrag, Macromolecules, to be submitted.